AUTHOR(S): MUHAMMAD-SUKKI, F., ABU-BAKAR, S.H., RAMIREZ-INIGUEZ, R., MCMEEKIN, S.G., STEWART, B.G., SARMAH, N., MALLICK, T.K., MUNIR, A.B., YASIN, S.H.M. and RAHIM, R.A.

TITLE: Mirror symmetrical dielectric totally internally reflecting concentrator for building integrated photovoltaic systems.

YEAR: 2014

Publisher citation: MUHAMMAD-SUKKI, F., ABU-BAKAR, S.H., RAMIREZ-INIGUEZ, R., MCMEEKIN, S.G., STEWART, B.G., SARMAH, N., MALLICK, T.K., MUNIR, A.B., YASIN, S.H.M. and RAHIM, R.A. 2014. Mirror symmetrical dielectric totally internally reflecting concentrator for building integrated photovoltaic systems. Applied energy [online], 113, pages 32-40. Available from: https://dx.doi.org/10.1016/j.apenergy.2013.07.010

OpenAIR citation: MUHAMMAD-SUKKI, F., ABU-BAKAR, S.H., RAMIREZ-INIGUEZ, R., MCMEEKIN, S.G., STEWART, B.G., SARMAH, N., MALLICK, T.K., MUNIR, A.B., YASIN, S.H.M. and RAHIM, R.A. 2014. Mirror symmetrical dielectric totally internally reflecting concentrator for building integrated photovoltaic systems. Applied energy, 113, pages 32-40. Held on OpenAIR [online]. Available from: https://openair.rgu.ac.uk

Mirror Symmetrical Dielectric Totally Internally Reflecting Concentrator for Building Integrated Photovoltaic Systems

Firdaus Muhammad-Sukki [a,b,*], Siti Hawa Abu-Bakar [a,c], Roberto Ramirez-Iniguez [a], Scott G McMeekin [a], Brian G Stewart [a], Nabin Sarmah [d], Tapas Kumar Mallick [d], Abu Bakar Munir [e], Siti Hajar Mohd Yasin [f], Ruzairi Abdul Rahim [g]

[a] School of Engineering & Built Environment, Glasgow Caledonian University, 70 Cowcaddens Road, Glasgow, G4 0BA Scotland, United Kingdom
[b] Faculty of Engineering, Multimedia University, Persiaran Multimedia, 63100 Cyberjaya, Selangor, Malaysia
[c] Universiti Kuala Lumpur British Malaysian Institute, Batu 8, Jalan Sungai Pusu, 53100 Gombak, Selangor, Malaysia
[d] College of Engineering, Mathematics and Physical Sciences, University of Exeter, Penryn, Cornwall, TR10 9EZ, United Kingdom
[e] Faculty of Law, University of Malaya, 50603 Kuala Lumpur, Malaysia
[f] Faculty of Law, Universiti Teknologi MARA, 40450 Shah Alam, Malaysia
[g] Faculty of Electrical Engineering, Universiti Teknologi Malaysia, 81300 UTM Skudai, Johor, Malaysia

* Corresponding Author. Tel: +44(0)141 331 8938, Fax: +44(0)141 331 3690
E-mail: firdaus.muhammadsukki@gcu.ac.uk/firdaus.sukki@gmail.com

Abstract: This paper describes a novel type of solar concentrator – a mirror symmetrical dielectric totally internally reflecting concentrator (MSDTIRC). This new concentrator type has been designed to satisfy the following objectives: (i) to provide optimum gain in two different planes, therefore increasing the electrical output of a solar photovoltaic (PV) system, and (ii) to reduce the amount of the PV cell material needed, hence minimising the cost of the system. The concentrator is capable of having two different acceptance angles on different planes. The procedure of designing an MSDTIRC is explained and the geometrical properties are analysed in detail. In addition, the optical concentration gain is presented for various angles of incidence. Through simulation results, it is demonstrated that the MSDTIRC provides significant optical concentration gain within its acceptance angle, as high as 13.64 when compared with non-concentrating solar cell. It can be concluded that the MSDTIRC can be an alternative way to produce a low cost solar PV system and can be chosen as an alternative design for the BIPV systems.

Keywords: solar photovoltaic; solar concentrator; mirror symmetrical dielectric totally internally reflecting concentrator.

1. Introduction

Solar photovoltaic (PV) is one of the renewable energy technologies that has great potential in supplying the world's energy needs. According to a statistic from BP Global [1], the total installed capacity of solar PV around the globe in 2012 reached 100.1 GW, as presented in Figure 1. Around 68.4% of the installations were carried out in Europe, 8.2% in North America with the remaining balance found in other parts of the world. The rising trend of solar PV installation in many countries is mainly catalysed by the implementation of a financial incentive known as the feed-in tariff (FiT) scheme, which is currently enacted in more than 80 countries [2].

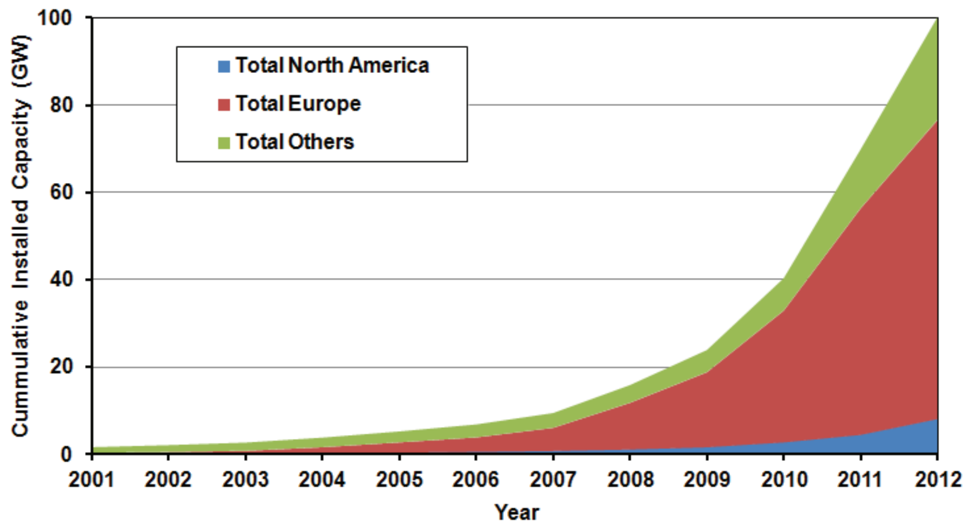

Figure 1: Cumulative installed capacity of solar PV worldwide in 2011. Adapted from [1].

The International Energy Agency (IEA) identified potential in integrating solar PV into the architectural design of roofs and facades for all types of building. A study [3] was conducted by the IEA to assess the prospect of building integrated photovoltaic (BIPV) systems in 14 selected countries. The study concluded that there is a BIPV area potential totalling approximately 23 billion m^2 and could generate about 3 PWh annually. According to another study by Oliver and Jackson [4], BIPV systems could offer additional advantages when compared with centralised solar PV plant which include the following:

i. Eliminate the cost of land acquisitions and the cost of support structures since the PV panels are mounted/replacing the building structure. The cabling cost could also be reduced since all buildings have access to the grid, unlike an isolated PV site.

ii. The electricity generated by BIPV systems could be consumed in the building itself, which minimises the losses due to the transmission and distribution of electricity. A reduction in the electricity bill could be achieved since the electricity generation coincides with the peak electricity demand during the day.

iii. The integration of PV panel substitutes parts of the building (e.g. roof, window, facade), eliminating the need for other building materials, which can be costly.

In the last decade, there has been a significant rise in the use of solar concentrators for BIPV applications, including sky lights, double glazing windows and solar blinds [5]-[7]. A solar concentrator is a device that allows the collection of sunlight from a large area and focuses it on a smaller receiver or exit [8]. The concentrator is aimed at reducing the usage of expensive PV material, hence reducing the overall cost of the system [5].

One example is the luminescence solar concentrator (LSC). With the ability to make full use of direct and diffuse sunlight, LSCs have the potential to replace windows and building facades. However, their low efficiency (the highest conversion efficiency is only 7.1% [9]) makes them less attractive for electricity generation, particularly if a homeowner wants to take full advantage of the FiT scheme.

Another concentrator type, called the asymmetrical compound parabolic photovoltaic concentrator (ACPPVC), was demonstrated by Mallick et al. [10]. These concentrators are made from reflective materials with strips of solar cell connected in series and attached at the exit aperture of the concentrators. Their experimental results indicate that this concentrator managed to increase the maximum electrical output power by 62% when compared with a similar system without a concentrator [10]. The panel could also be mounted on the roof or replace the wall of a building.

The asymmetrical compound parabolic concentrator (CPC) extrusion is another example employed by the Photovoltaic Facades of Reduced Cost Incorporating Devices with Optically Concentrating Elements (PRIDE) project which was carried out in the late 1990s [7],[11]. The asymmetrical CPC is made from dielectric materials. The first generation of PRIDE technology concentrators produced 2.3 times more electrical output when compared with a flat plate conventional solar PV [11]. However, it has disadvantages in terms of durability and instability of the dielectric material under long term outdoor characterisation [12]. This is because the concentrators were produced from casting processes which are prone to UV degradation [12]. With the aim of large scale production, durability and reduction in weight and cost, the second generation PRIDE design was developed in 2006 [12]. The prototype of the improved design was a 3 kWp PV concentrator module and was built using injection moulding processes. This design is suitable for building facade integration. When compared with a non-concentrating system, this prototype achieves a 2.01 output power gain. It is projected that the second generation PRIDE technology system could reduce the module cost by approximately 40% [12].

Recently, Sellami et al. developed a novel static 3D concentrator called the Square Elliptical Hyperboloid (SEH) for BIPV applications [5]. This concentrator has an elliptical entry aperture, hyperbolic side profiles and a square or rectangular exit aperture where a PV cell is attached. It has the potential to be integrated into double glazed windows. With a concentration value of 4x and acceptance angle of 120^o ($\pm 60^o$), an optical efficiency of 40% was recorded [5]. The large value of acceptance angle helps to eliminate the need for mechanical solar tracking.

Clive has also proposed an alternative design for BIPV systems known as SolarBrane which comprises of extrusions of dielectric totally internally reflecting concentrators (DTIRCs) [13]. SolarBrane can reduce the usage of PV material by 70% while maintaining the same output power when compared with a traditional solar panel [14]. The use of DTIRCs has the potential of reducing the cost of implementation of conventional solar PV systems by 40% [14].

Chemisana et al. [15] on the other hand investigated a holographic solar concentrator for the BIPV application. This concentrator is capable of diffracting light in the spectral bandwidth to which the cell presents the highest sensitivity - allowing the PV cell to be protected from overheating [15]. It is reported that the holographic concentrator managed to increase the efficiency of the PV cell by 3% [15].

This paper proposes a new type of solar concentrator for use in BIPV systems. This concentrator is known as a mirror symmetrical dielectric totally internally reflecting concentrator (MSDTIRC). Section 2 explains the steps involved in producing the design, and the geometrical properties of the MSDTIRC are presented in Section 3. The optical concentration gain analysis is carried out in Section 4 prior to presenting the experimental result of the optical gain of the concentrator in Section 5. The annual output prediction of implementing the MSDTIRC in Malaysia is discussed in Section 6. Next the potential of MSDTIRC is outlined in Section 7. Conclusions are presented at the end of the paper.

2. Design of MSDTIRC

The MSDTIRC is a new variation of the DTIRC. This concentrator is able to achieve different field of views on different planes. In contrast to the rotational axis symmetrical DTIRC proposed by Ning et al. [16], this novel design generates a mirror symmetry design in four axes parallel to the base of the concentrator.

The MSDTIRC uses the DTIRC based on the phase conserving method (PCM) as the design's foundation. The MSDTIRC requires a number of input parameters, which are listed below; the total height of the concentrator, (*HTot*), the trial front surface arc angle (φ), the acceptance angle on the x-axis ($\theta_{a\text{-}x}$), the acceptance angle on the z-axis ($\theta_{a\text{-}z}$), the length of the PV cell (L_{PV}), the width of the PV cell (W_{PV}), the trial length of the entrance aperture (d_1), the index of refraction of the material (n) and the number of extreme rays (N).

A MATLAB® based program has been developed to create the MSDTIRC. The algorithm is summarised in Figure 2. First, a 2D design is calculated based on the input variables, with the initial acceptance value equal to the acceptance angle on the x-axis ($\theta_{a\text{-}x}$). The computer program calculates the trial height, which is later used to calculate the coordinates of the side wall. This calculation takes into account the number of extreme rays entering the concentrator at the critical angle. Once it is completed, the program compares the trial entrance aperture with the calculated aperture. A new entrance aperture is then computed from the difference between the two apertures. A number of iterations take place until the difference between both apertures is within an acceptable error value. The calculated total height of the concentrator is then compared with the desired total height. The total height is adjusted by varying the front surface arc angle until the difference between the total heights is within an acceptable value. The process is repeated to get the next 2D design, with each new design computed by incrementing the acceptance angle and the exit diameter accordingly using the value of $\Delta\theta_a$ and Δd_0 respectively. The process stops when a 180^o rotation around the y-axis is completed.

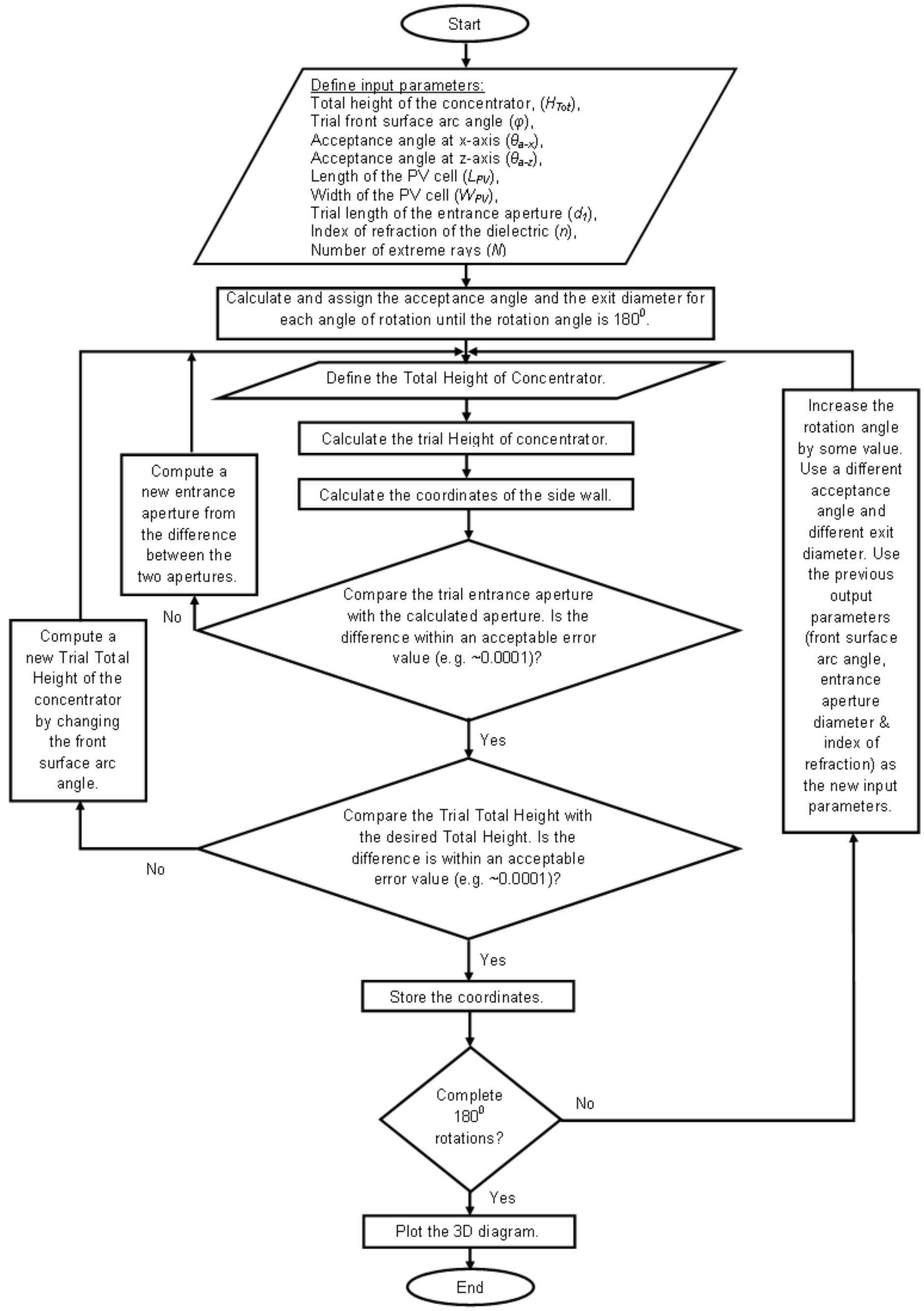

Figure 2: The flowchart of producing an MSDTIRC.

Figure 3 illustrates of the steps to produce the MSDTIRC, starting from position (plane) 1. For each position, a different profile is generated having different front surface arc angle and positioned at a different location of the exit aperture.

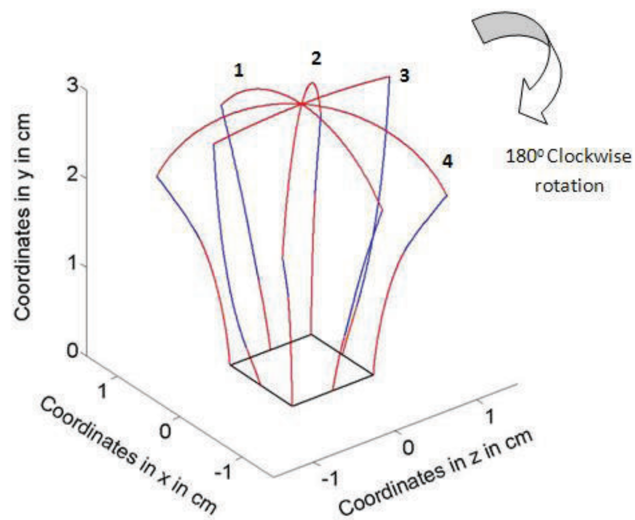

Figure 3: Illustration on how to generate the MSDTIRC from the 2D DTIRC design.

The MSDTIRC shown in Figure 4 is generated by selecting the total height *HTot* of 3.0 cm, an acceptance angle $\theta_{a\text{-}x}$ in the x-axis of $\pm 30^{o}$, an acceptance angle $\theta_{a\text{-}z}$ in the z-axis of $\pm 40^{o}$ and a refractive index n of the dielectric material from which the optical element is constructed with a value of 1.5. Unlike the 3-D rotationally symmetry DTIRC that has a smooth dome shape entrance front surface, this design has a sectored front surface with four axis of mirror symmetry (see Figure 3(d)). Depending on the selection of input parameters, the front surface will be different from each design. Another important characteristic of this concentrator is its square exit aperture, as presented in Figure 3(e). According to Sellami and Mallick [17], from the manufacturing point of view, it is desirable and easier to fabricate a square/rectangular cell, unlike a circular cell employed in a rotationally symmetry design.

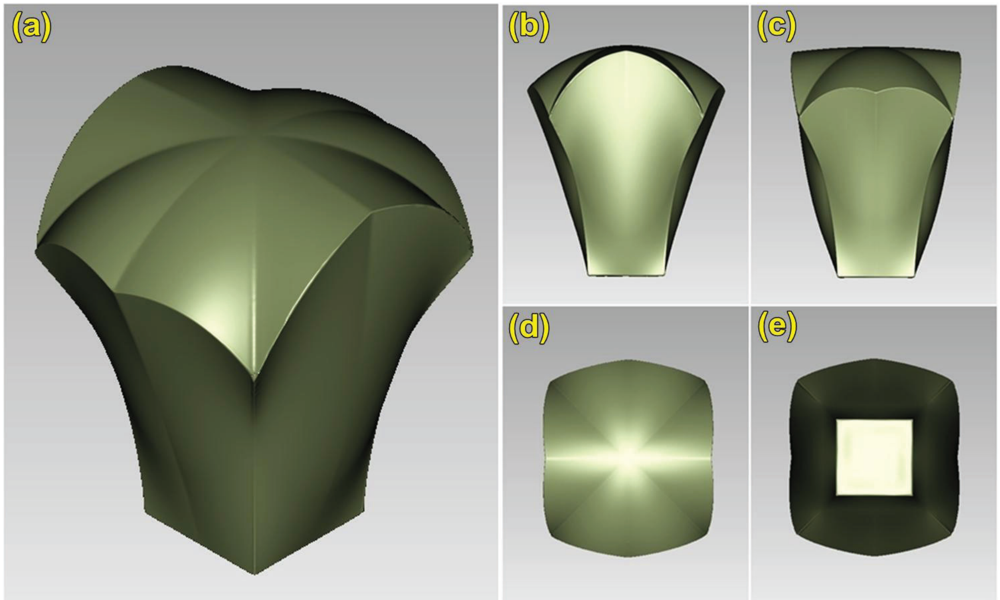

Figure 4: MSDTIRC (*HTot* = 3.0 cm, $\theta_{a\text{-}x} = \underline{+}30^{o}$, $\theta_{a\text{-}z} = \underline{+}40^{o}$, $n = 1.5$), where (a) is the isometric view; (b) is the side view 1; (c) is the side view 2; (d) the aerial view, and (e) is the bottom view of the concentrator.

3. Geometrical Concentration Gain Analysis

This subsection analyses the impact that changing the total height and the index of refraction of the material has on the geometrical concentration gain of the MSDTIRC. This is useful to predict the final output gain based on the input parameters especially from the manufacturing point of view. Often, a high output gain is desirable, but this normally translates into a larger structure [13] and increases the material cost [14]. Therefore some trade off must be met, i.e. by choosing the appropriate gain while at the same time keeping the total cost as low as possible. The geometrical concentration gain of a 3D concentrator is defined as the ratio of the entrance aperture to the exit aperture of the concentrator [18].

It is not possible to know the direct relationship between the geometrical concentration gain, the front surface arc angle, and the acceptance angle in an MSDTIRC design. This is because it uses a range of acceptance angles in a single design and the arc angle varies throughout its top surface. However, owing to the fact that the MSDTIRC's design strategy is based on the DTIRC design, it should mimic its characteristics. It has been shown that a DTIRC's geometrical concentration gain is inversely proportional to both the arc angle and the acceptance angle [13],[14]. By having a higher acceptance angle, the total height of the concentrator greatly reduces. To further simplify the analysis in this subsection, the MSDTIRC analysis is undertaken in three groups:

- Group 1, where the total height[1] is between 6.4 cm to 6.8 cm and the acceptance angle[2] is between ±15° to ±25°.
- Group 2, where the total height is between 4.5 cm to 4.9 cm and the acceptance angle is between ±20° to ±30°.
- Group 3, where the total height is between 2.9 cm to 3.2 cm and the acceptance angle is between ±30° to ±40°.

The relationship between the geometrical concentration gain and the total height (for each group of MSDTIRCs) using various refractive indices[3] is shown in Figures 5 to 7. Figure 5 shows the gain for the MSDTIRCs from Group 1, which have the highest gain range of between 11 and 15. The gain in Group 2 ranges from 7 to 10 as presented in Figure 6. The gain reduces to between 3.5 and 5.5 for Group 3, as indicated in Figure 7. Comparing these three groups, it can be seen that as the total height and the acceptance angle are changed, the geometrical concentration gain varies greatly. The gain is also inversely proportional to the acceptance angle, which is as expected [13]. However, looking closely at the MSDTIRCs within the same group, the difference in height has a very small effect on the gain. It is also possible to conclude from the three graphs that MSDTIRCs fabricated using higher refractive index materials produce higher gains than similar MSDTIRCs made from materials having a lower refractive index.

---

[1] A typical solar panel has a thickness of between 2.5 cm and 7.5 cm [19],[20]. If a new panel incorporates the MSDTIRCs, the total height of MSDTIRC and the glass covers would be constructed within this range.

[2] The range of acceptance angles can be designed according to the requirement. For this paper, this value is chosen to be from ±15° onwards to cater for the variation of seasonal sun path in Europe [21].

[3] This range of indices of refraction is the typical range for concentrator materials and optical lenses. Some examples of concentrator materials are PMMA (n = 1.491), Acrylic glass (n = 1.490 - 1.492) and ZEONEX (n = 1.509), while the example of optical lenses are Lithosil-Q (n = 1.45), H-QK1 (n = 1.47), K11 (n = 1.50) and BK8 (n = 1.52). In this paper, an optical system design software called ZEMAX® is used for simulations and ray tracing analysis. This software contains a variety of optical glasses that can be chosen for optical simulations, as presented later in Section 4.

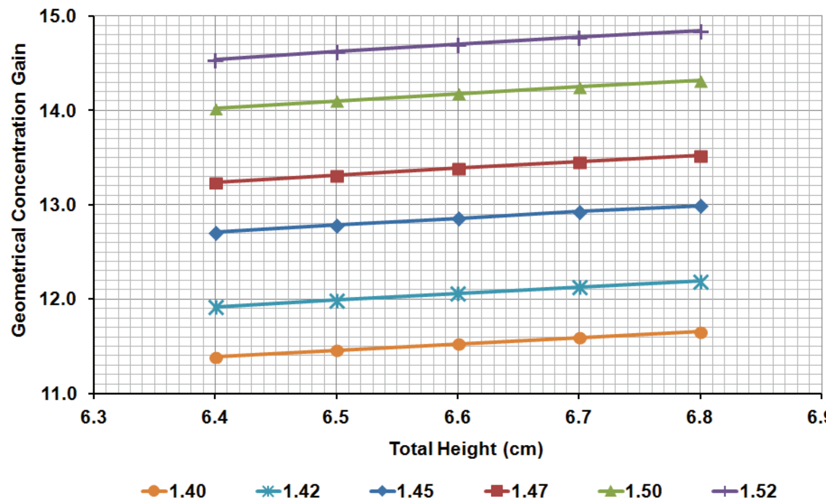

Figure 5: Geometrical Concentration Gain of Group 1 (n = 1.40 to 1.52).

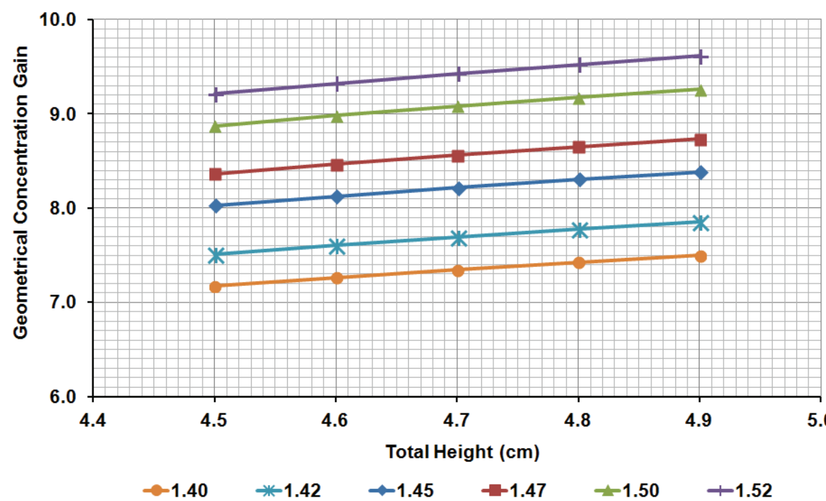

Figure 6: Geometrical Concentration Gain of Group 2 (n = 1.40 to 1.52).

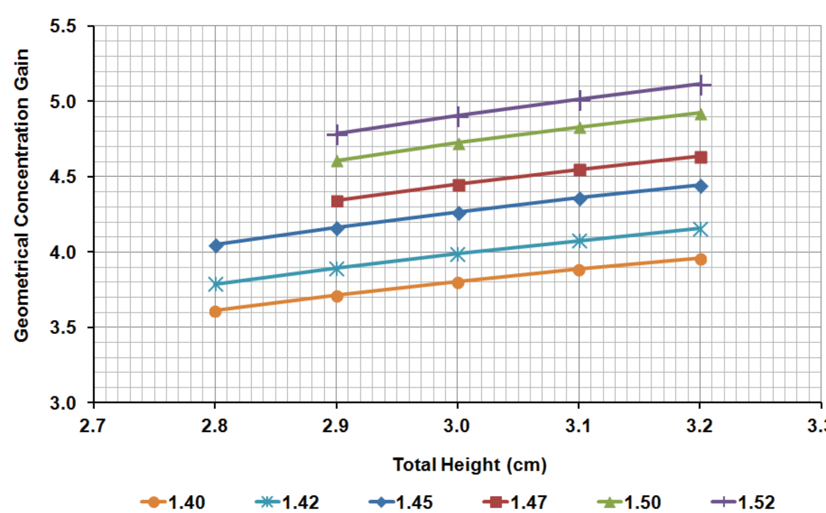

Figure 7: Geometrical Concentration Gain of Group 3 (n = 1.40 to 1.52).

It is also interesting to note that there is no data available for an MSDTIRC with a total height of 2.8 cm with index of refraction of 1.47, 1.50 and 1.52 (see Figure 7). This is because the MSDTIRC with these particular parameters is physically impossible to fabricate as they do not fulfil the necessary DTIRC conditions [16].

Therefore, depending on the desired design, some trade-offs may need to be made. For example, it may be possible to achieve a smaller solar concentrator with wider field of view but accepting a smaller gain, or to use a concentrator with a smaller field of view and achieving a higher gain, but at the cost of a larger structure.

4. Optical Concentration Gain Analysis

The optical concentration gain is defined as the ratio of the irradiance at the photo detector with a concentrator placed in front of it to that of a photo detector without the concentrator [22]. Based on the geometrical gain analysis presented in Sections 3, it is possible to conclude that the optical concentration gain will present a similar trend. The purpose of the analysis in this section is to evaluate the variation of optical concentration gain of the MSDTIRC at different angles of incidence.

The optical concentration gain variation is useful to predict the output performance of the MSDTIRC when the sun is considered as the light source. The angle variation of the incident rays along the x-axis represents the seasonal changes of the sun angle while the angle variation of the incident rays along the z-axis represents the daily sun path. To simplify the analysis, only one design of MSDTIRC is chosen from each group. The index of refraction of the material chosen for this analysis is 1.5.

Three pieces of software are used to conduct this simulation. Because of the complexity of the design, MATLAB is used to generate the surface coordinates (point cloud) of any MSDTIRC, which are then imported into GeoMagic® or AutoCAD software, to generate a computer-aided design (CAD) model from which a Standard ACIS Text (SAT) format file model is obtained, as illustrated in Figure 3. The SAT file is then used in an optical system design software called ZEMAX® to conduct the ray tracing analysis.

The ray tracing analysis is presented in Figure 8. A square power source is chosen to produce one million parallel rays and is configured to produce an incoming power of 1,000 W. The size of the source is large enough to cover the entirety entrance aperture of the concentrator at all angles of incidence. The CAD model of the MSDTIRC is placed at a distance of 35cm from the source and a photo detector is attached at the exit aperture of the concentrator.

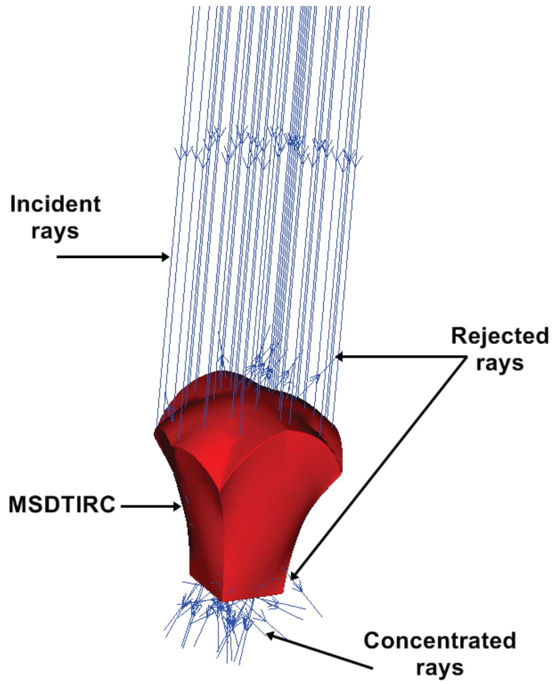

Figure 8: Ray tracing analysis conducted in ZEMAX®.

First, the rays are fired perpendicular to the photodetector without the incorporation of the concentrator and the total power and the numbers of rays detected at the photo detector are recorded. The step is repeated by increasing the angle of incidence by 5^{o} until a value of 50^{o} is reached. Next, an MSDTIRC is "attached" to the photo detector (placed in between the source and the photo detector) and both steps are repeated. The analysis is carried out to investigate the optical concentration gain at both the x and the z-axes.

Similar to the analysis in [5] and [22], it has been found in this analysis that the optical gain reaches a maximum value when the rays are fired at normal incidence, and this value reduces gradually when the angle of incidence increases until it is equal to the value of the acceptance angle. Beyond the acceptance angle of the concentrator, the gain should decrease greatly. Figures 9 to 11 show the optical performance of the MSDTIRCs for Groups 1, 2 and 3 design respectively.

In Figure 9, the maximum optical concentration gain of the MSDTIRC with a total height of 6.5 cm is 13.54. By increasing the angle of incidence of the rays along the x and z-axis, the optical concentration gain drops dramatically. The gain reduces to about 24% (of the maximum) when the angle of incidence reaches the acceptance angle of $\pm 15^{o}$ along the x-axis and to about 10% when the angle of incidence reaches the acceptance angle of $\pm 25^{o}$ along the z-axis. The gain drops to almost 0 when the angle of incidence is $\pm 30^{o}$ or more.

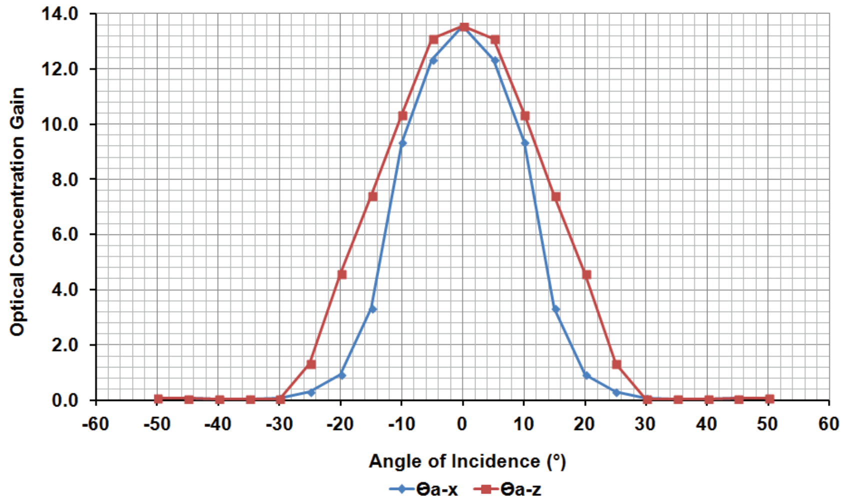

Figure 9: Optical concentration gain of Group 1 with *HTot* = 6.5 cm, and *n* = 1.50.

Figure 10 shows the optical concentration gain of the sample from Group 2. When the rays are fired at normal incidence, the maximum optical concentration gain of the MSDTIRC with a total height of 4.5 cm is 8.62. An increase in the angle of incidence of the rays along the x and z-axis reduces the optical concentration gain, which drops considerably. The gain reduces to roughly 14% when the angle of incidence reaches the acceptance angle of $\pm 20^{o}$ along the x-axis and to about 6% when the angle of incidence reaches the acceptance angle of $\pm 30^{o}$ along the z-axis. The gain drops to almost 0 when the angle of incidence is $\pm 40^{o}$ or more.

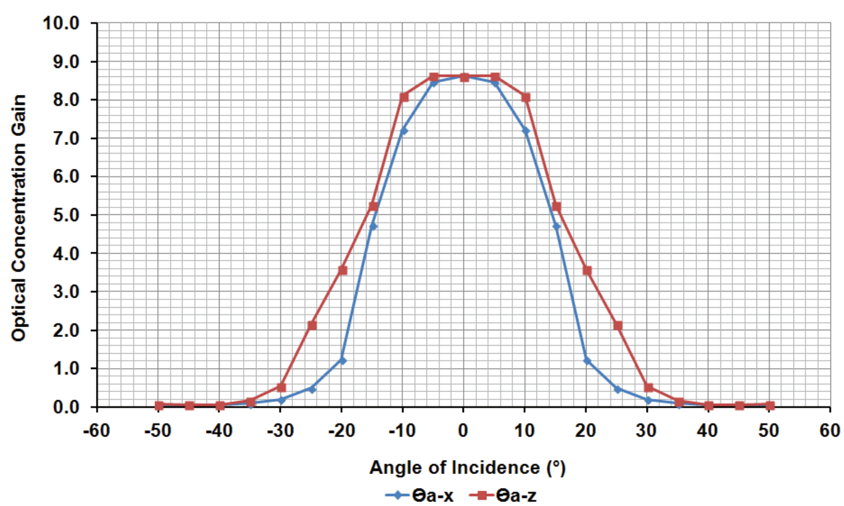

Figure 10: Optical concentration gain of Group 2 with *HTot* = 4.5 cm, and *n* = 1.50.

A similar trend is also observed for the MSDTIRCs from Group 3. In Figure 11, the peak value of optical concentration gain of the MSDTIRC with a total height of 3.0 cm is 4.43. An increase in the angle of incidence of the rays along the x and z-axes reduces the optical concentration gain gradually. The gain reduces to 8% when the angle of incidence reaches the acceptance angle of $\pm 30^{\circ}$ along the x-axis and to about 3% when the angle of incidence reaches the acceptance angle of $\pm 40^{\circ}$ along the z-axis. No significant gain is recorded when the angle of incidence is $\pm 50^{\circ}$ or more.

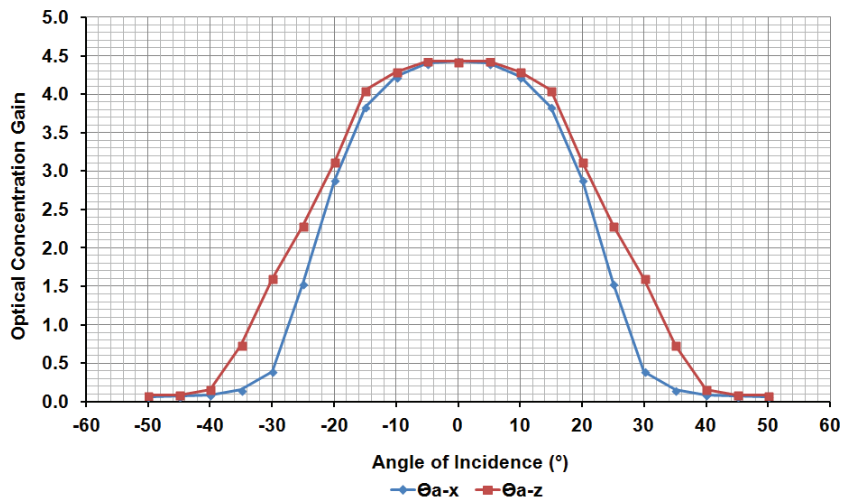

Figure 11: Optical concentration gain of Group 3 with *HTot* = 3.0 cm, and *n* = 1.50.

From the analysis, it can be concluded that within the desired acceptance angle, the MSDTIRC could provide significant optical concentration gain within a solar panel design, with the highest value recorded when the rays are at normal incidence. Outside the acceptance angle, the gain is reduced significantly.

Another factor that needs consideration when choosing the MSDTIRC is the distribution of irradiance concentration on the solar cell. Any non-uniformity of distribution of the irradiance on the cells reduces their efficiency [5]. The concentration of the irradiance on the solar cell due to the introduction of MSDTIRC is observed while investigating the optical concentration gain analysis. Figure 12 shows the distribution of irradiance as a result of using the three concentrators at normal incidence.

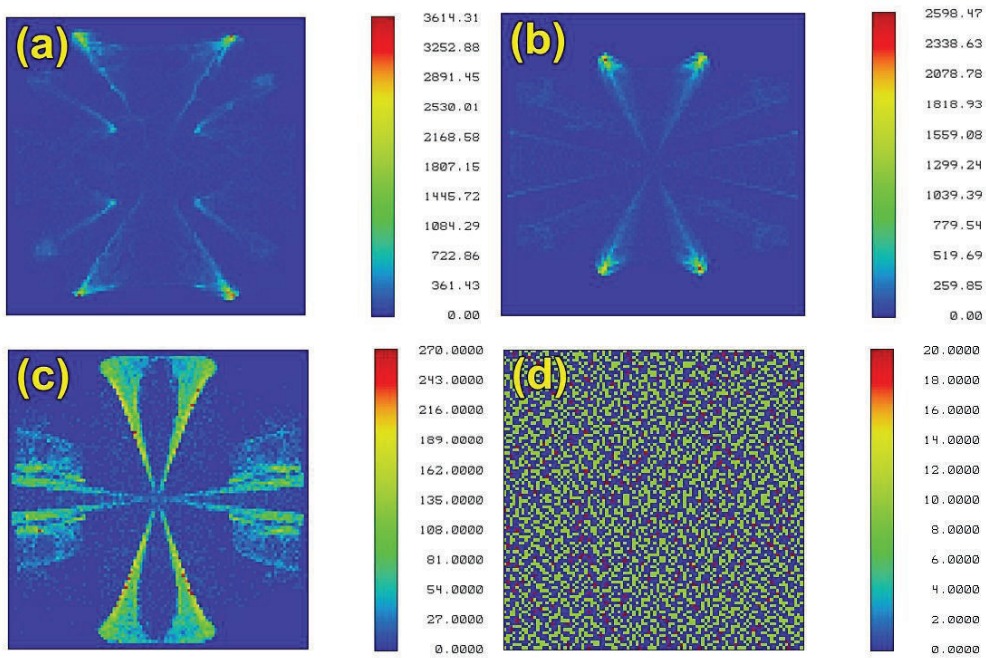

Figure 12: Photodetector's results obtained from the ZEMAX® simulation of concentration distribution at the cell of (a) Group 1 design; (b) Group 2 design; (c) Group 3 design, and (d) flat solar cell. The unit is recorded in W/cm^2.

The simulation shows an even irradiance distribution on a normal flat solar cell, with a peak irradiance of 20 W/cm^2, as indicated in Figure 13(d). However, the concentration of light for Group 1 and 2 designs are concentrated mostly at four small areas of the cell, with the maximum concentration reaching 181x and 130x when compared with the flat solar cell. As for the Group 3 design, it produces a more uniform concentration distribution when compared with the designs from Group 1 and 2, with a maximum of 14x with respect to the flat solar cell. A high concentration of power increases the solar cell temperature and significantly reduces the cell performance [5]. Any designs that required higher gain must incorporate a system to reduce the cell's temperature (either using air or water), and one of the solutions is to implement the hybrid/thermal system that utilises the co-generated heat to produce hot water [23].

5. Experimental validation[4]

An MSDTIRC from Group 3 was fabricated for experimental purposes. This has a total height of 3.0 cm and an acceptance angle of ±30^o along the x-plane and ±40^o along the z-plane. The geometrical concentration gain of the concentrator is 4.9069. The design was produced using

[4] A more detailed information regarding the fabrication process and extensive indoor and outdoor experiments of the MSDTIRC is covered in Ref [24].

material 6091 (manufactured by Renishaw PLC), which was selected because of its rigidity, water clarity and transparency. The material can also withstand high temperatures (up to 75^{o}C), is UV stable, it has a refractive index of 1.515 and a transmissibility of 93.7%.

The MSDTIRC prototype has been placed beneath a sun simulator. The sun simulator is set to exhibit an irradiance of 1,000 W/m^2, when the room temperature is 25^{o}C. Instead of changing the rays' angle, the MSDTIRC is mounted on a variable slop base, where the base can be tilted accordingly. The tilt angle is measured accurately using a digital tilt meter. The measurement of the short circuit current is taken, for an angle of inclination starting from 0^{o} to 50^{o}, with intervals of 5^{o}.

The opto-electronic gain of the concentrator is obtained by dividing the MSDTIRC's short circuit current with the flat solar cell's short circuit current [16], and is plotted in Figure 13. From Figure 13, it is observed that within the acceptance angles of the MSDTIRC, the opto-electronic gain is always more than 1.2 when compared with the flat solar cell, where the peak value calculated from the experiment is 4.17. The corresponding peak value from the simulation is the peak value from the optical concentration gain, i.e. 4.59, indicating a deviation of about 9%. The result from the experiment shows good agreement with the simulation data. Some of the possible reasons for the deviation between the experimental and simulation values include manufacturing errors, such as uneven surfaces of the entrance aperture and over polishing on the profile of the side wall, misalignment between the exit aperture of the concentrator and the solar cell, and reflection on the front surface of the MSDTIRC.

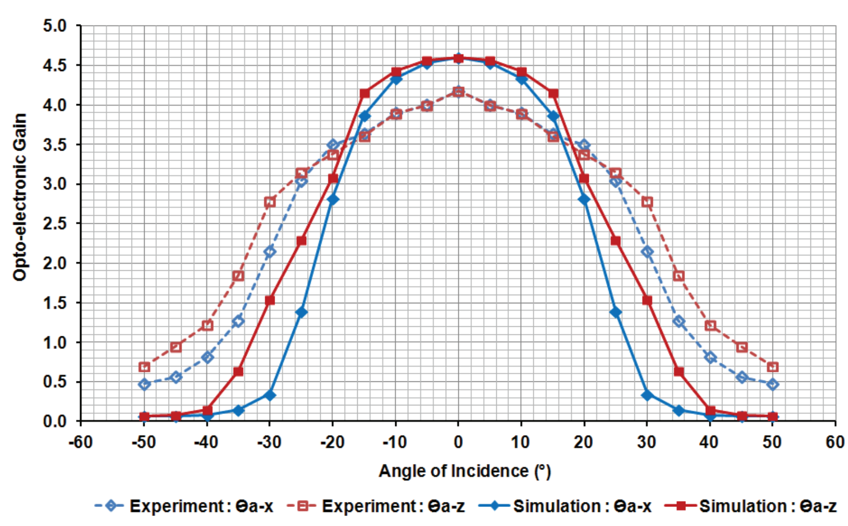

Figure 13: Opto-electronic gain of the MSDTIRC.

6. Annual output prediction

It is possible to predict the annual output (in kWh) from the MSDTIRC[5] panel (see Figure 14) and a conventional PV skylight (without concentrator) under Malaysia's environment. This comparison is carried out to evaluate the panels' performance based on the square meter of the PV material used in each panel. This analysis is carried out according to these assumptions, which are: (i) each panel has the length and width of 118.62 cm and 79.42 cm respectively, with cell conversion efficiency of 17.32%[6]; (ii) the samples are installed in Kuala Terengganu, Malaysia (103°25'); (iii) the samples are mounted on a south facing rooftop at an angle of 103^{o} from the vertical to match the longitude of the site, and (iv) no mechanical tracking system is employed by the system. The simulation is carried out using ZEMAX® to evaluate the opto-electronic gain of the samples. Based on the average daily solar irradiance data in Kuala Terengganu, Malaysia [25], the variation of sun path throughout the year [21] and the daily opto-electronic gain from the ZEMAX® simulation, the energy yield from both samples are calculated.

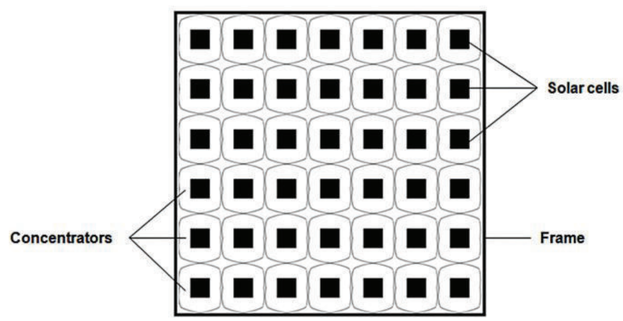

Figure 14: Aerial view of the arrangement of MSDTIRCs in a module.

Figure 15 shows the annual output from the MSDTIRC panel and the traditional PV skylight. It can be seen that the MSDTIRC could increase the electrical output by 2.16 times when compared with amount generated by the traditional PV skylight, generating about 107.59 kWh per year. However, the predicted annual energy only indicates the comparison in terms of electricity generation. Other benefits of utilising an MSDTIRC panel should also be taken into account; especially in terms of illumination and the possibility of generating hot water and space heating,

---

[5] The MSDTIRC used in the panel is from Group 3 (($HTot$ = 3.0 cm, $\theta_{a-x} = \pm 30^{o}$, $\theta_{a-z} = \pm 40^{o}$, n = 1.5).

[6] This is based on the efficiency of the cell used during the experiments.

which will further reduce the energy requirement in a building.

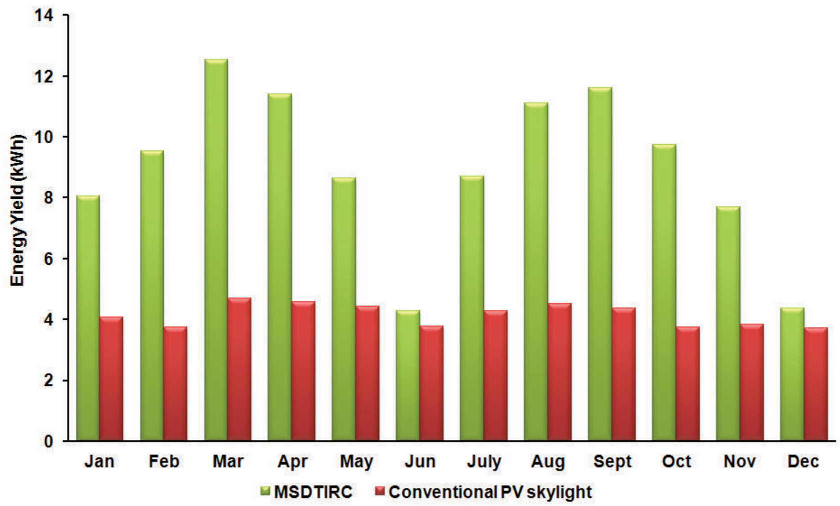

Figure 15: Comparison between the MSDTIRC panel and the traditional PV skylight.

7. Advantages of the MSDTIRC

The MSDTIRC-PV system offers several advantages when compared with the conventional flat plate panel. These are:

i. It utilises only a fraction of the silicon solar cell in the design – as little as only 10% (depending on the design) when compared to the normal solar panel. It is understood the silicon wafers covers immense fraction of the total cost of the module, typically between 40% and 60% depending on the type of solar cell. [17],[26].

ii. The large entrance aperture allows the rays within the acceptance angle of the concentrator to be concentrated on the solar cell hence increasing the electrical output. The gain increment offset a reduction in terms of the size of the cell.

iii. The usage of a square solar cell is desirable and easier to fabricate unlike the circular cell in the rotationally symmetry design [26].

iv. It is constructed from transparent dielectric material by using a moulding technique, which is cheaper than the cost of displaced silicon solar cell and much easier to mass produce hence minimising the manufacturing cost.

v. For rays impinging on the entrance aperture outside the acceptance angle range and in between the entrance aperture of the concentrators, these rays could pass through the transparent material providing natural illumination for a building, which could potentially reduce the energy consumption and electricity cost for lighting purposes.

vi. The large acceptance angle also helps to eliminate the need for mechanical tracking. Tracking systems often consume electrical energy and are normally associated with PV power plant [8].

vii. Small compact dielectric concentrators coupled with small solar cells produce more economical and practical designs than larger and heavier dielectric concentrators [27].

viii. The concentrating PV (CPV) system works better and more efficiently when it is operated in a hybrid/thermal system application, which generates both electricity and hot water at the same time [23].

ix. When coupled with the FiT scheme, the total cost reduction of the system enables the participant(s) to gain more total profit, a higher return on investment, and a shorter payback period [28],[29].

Conclusions

This paper explores the MSDTIRC, a new type of DTIRC. The method to produce an MSDTIRC has been explored and the geometrical analysis of the MSDTIRC is presented in detail. Through simulation results, it has been demonstrated that this MSDTIRC provides significant optical concentration gains within its acceptance angle. In this paper, it could reach up to 13.64 when compared with non-concentrating solar cell. This is verified in through experimental work and a deviation of only 9% of the peak value is recorded. It can be concluded that the MSDTIRC can be an alternative way to produce a low cost solar PV system and can be chosen as an alternative design for the BIPV systems.

Acknowledgments

The authors would like to thank Glasgow Caledonian University, the Scottish Funding Council and Yayasan TM for funding this research activity.

References

[1]. BP Global, 2013. Statistical Review of World Energy 2013. BP Global, U.K.

[2]. Renewable Energy Policy Network for the 21st Century (REN21), 2013. Renewables 2013 Global Status Report. REN21, Paris.

[3]. International Energy Agency (IEA), 2002. Potential for building integrated photovoltaics. Report IEA-PVPS T7-4:2002 (Summary), IEA.

[4]. Oliver M & Jackson T, Energy and economic evaluation of building-integrated photovoltaics. Energy 2001; 26: 431-439.

[5]. Sellami N, Mallick TK & McNeil DA. Optical characterization of 3-D static solar concentrator. Energy Conversion and Management 2012; 64: 579-586.

[6]. Baig H & Mallick TK, Challenges and opportunities in concentrating photovoltaic research. Modern Energy Review 2011; 3(2): 20-26.

[7]. Norton B, Eames PC, Mallick TK, Huang MJ, McCormack SJ & Mondol JD. Enhancing the performances of building integrated photovoltaics. Solar Energy 2011; 85(8): 1629-1664.

[8]. Muhammad-Sukki F, Ramirez-Iniguez R, McMeekin SG, Stewart BG & Clive B. Solar concentrators. International Journal of Applied Sciences 2010; 1(1): 1-15.

[9]. Slooff LH, Bende EE, Burgers AR, Budel T, Pravettoni M, Kenny RP, Dunlop ED & Buchtemann A. A luminescent solar concentrator with 7.1 % power conversion efficiency. Physica Status Solidi (RRL) 2008; 2(6): 257-259

[10]. Mallick TK, Eames PC & Norton B. Non-concentrating and asymmetric compound parabolic concentrating building façade integrated photovoltaics: An experimental comparison. Solar Energy 2006; 80(7): 834-849.

[11]. Zacharopoulos Z, Eames PC, McLarnon D & Norton B. Linear dielectric non-imaging concentrating covers for PV integrated building facades. Solar Energy 2000; 68(5):439-452.

[12]. Mallick TK & Eames PC. Design and fabrication of low concentrating second generation pride concentrator, Solar Energy materials and Solar Cells 2007; 91(7):597-608.

[13]. Muhammad-Sukki F, Ramirez-Iniguez R, McMeekin SG, Stewart BG & Clive B. Optimised dielectric totally internally reflecting concentrator for the solar photonic optoelectronic transformer system: Maximum concentration method. In: Setchi R, Jordanov I, Howlett RJ & Jain LC, editors. Knowledge-Based and Intelligent Information and Engineering Systems 2010; 6279(4): 633-641.

[14]. Muhammad-Sukki F, Ramirez-Iniguez R, McMeekin SG, Stewart BG & Clive B. Solar concentrators in Malaysia: Towards the development of low cost solar photovoltaic systems. Jurnal Teknologi 2011; 55(1): 53-65.

[15]. Chemisana D, Collados MV, Quintanilla M & Atencia J. Holographic lenses for building integrated concentrating photovoltaics. Applied Energy 2013;110: 227-235.

[16]. Ning X, Winston R & O'Gallagher J. Dielectric Totally Internally Reflecting Concentrators. Applied Optics 1987; 26(2): 300–305.

[17]. Sellami N & Mallick TK. Optical efficiency study of PV crossed compound parabolic concentrator. Applied Energy 2013; 868-876.

[18]. Welford WT & Winston R. High Collection Nonimaging Optics. 1st edn. USA. Academic Press Inc. 2000.

[19]. Eco Expert, 2011. Last access on [16/07/2011]. Available from http://directory.theecoexperts.co.uk/manufacturer/kyocera

[20]. Energy & Environmental Ltd, 2011. Last access on [16/07/2011]. Available from http://www.energyenv.co.uk/solarmodulesmain.asp

[21]. Boxwell M. Solar electricity handbook. 1st edn. USA. Green Stream Publishing. 2010.

[22]. Muhammad-Sukki F, Ramirez-Iniguez R, McMeekin SG, Stewart BG & Clive B. Optimised concentrator for the Solar Photonic Optoelectronic Transformer: Optical concentration gain analysis. Proceedings of IET Renewable Power Generation Conference 2011; P4: 1-6.

[23]. Kumar R & Rosen MA. A critical review of photovoltaic-thermal solar collectors for air heating. Applied Energy 2011; 88: 3603-3614.

[24]. Muhammad-Sukki F, Abu-Bakar SH, Ramirez-Iniguez R, McMeekin SG, Stewart BG, Munir AB, Mohd Yasin SH, & Abdul Rahim R. Performance analysis of a mirror symmetrical dielectric totally internally reflecting concentrator for building integrated photovoltaic systems. Applied Energy 2013; 111: 288-299.

[25]. Muzathik AM, Wan Nik WMN, Samo K, & Ibrahim MZ. Hourly global solar radiation estimates on a horizontal plane. Journal of Physical Science 2010; 21(2): 51–66.

[26]. Mammo ED, Sellami N & Mallick TK. Performance analysis of a reflective 3D crossed compound parabolic concentrating photovoltaic system for building façade integration. Progress in Photovoltaic: Research and Applications 2012; http://dx.doi.org/10.1002/pip.2211.

[27]. Uemetsu T, Warabikaso T, Yazawa Y & Muramatsu S. Static micro-concentrator photovoltaic module with an acorn shape reflector. Proceedings of World Conference on Photovoltaic Solar Energy Conversion 1998; 1570-1573.

[28]. Muhammad-Sukki F, Munir AB, Ramirez-Iniguez R, Abu-Bakar SH, Mohd Yasin SH, McMeekin SG & Stewart BG. Solar photovoltaic in Malaysia: The way forward. Renewable and Sustainable Energy Reviews 2012; 16(7): 5232-5244.

[29]. Muhammad-Sukki F, Ramirez-Iniguez R, Abu-Bakar SH, McMeekin SG & Stewart BG. An evaluation of the installation of solar photovoltaic in residential houses in Malaysia: Past, present and future. Energy Policy 2011; 39(12): 7975–7987.